Eur. Phys. J. D **42**, 11–14 (2007)
DOI: 10.1140/epjd/e2006-00264-2

THE EUROPEAN PHYSICAL JOURNAL D

Low-energy electron scattering from copper

S.Y. Yousif Al-Mulla[a]

University of Borås, College of Engineering, Physics and Mathematics Group, 50190 Borås, Sweden

Received 24 October 2006 / Received in final form 7 November 2006
Published online 8 December 2006 –

Abstract. Differential cross sections for the elastic scattering of electrons from the ground states of copper for the configuration $3d^{10}4s$ and the excitation state ^{2}D with the configuration $3d^9 4s^2$ have been calculated. Local density approximations to the exchange and correlation potentials have been used in these calculations, and it is confirmed that Hara exchange coupled with a Hedin-Lundqvist electron-gas-type correlation potential joined to an adiabatic polarization potential gives good predictions for differential cross sections. A comparison of the calculated results with other experimental and theoretical data are presented and discussed.

PACS. 34.80.Bm Elastic scattering of electrons by atoms and molecules

1 Introduction

In previous work on elastic scattering of slow electrons from closed shell targets, Ne, Ar, Kr and Xe atoms [1,2] and from open shell targets, Mg and Ba [3], in which we employed various local-density approximations to the exchange and correlation potentials, we concluded that Hara exchange [4] coupled with a Hedin-Lundqvist [5] electron-gas-type correlation potential joined to an adiabatic polarisation potential, gives excellent predictions for phaseshifts and differential cross sections for closed-core rare-gas-atom systems, with well defined atomic radii, and open shell targets, specifically Mg and Ba atoms. The study of electron scattering from neutral atoms has provided a foundation of our theoretical understanding of the process.Very recently, Yousif Al-Mulla [6] has used the local density approximation to describe electron scattering from atoms and ions containing core holes, where the extension of electron scattering studies to charged ionic targets will yield insight into the atomic structure of ionized matter. This can lead to understand the technological potential of high-temperature plasmas, especially after the development of X-ray lasers [7]. The analysis of such plasmas requires knowledge of the processes of elastic scattering, excitation and ionization of atomic and ionic targets.

Interest in the field of electron scattering from copper has increased following the increase in interest to understand the copper vapour laser. The ground state of copper ($Z = 29$) has a single $4s$ electron outside a filled core with configuration $3d^{10}4s$. The lowest two excited states are the ^{2}D state with configuration $3d^9 4s^2$ and the ^{2}P state with configuration $3d^{10}4p$.

Experimental advances in this area have allowed the measurement of differential and integral cross sections for electron scattering from Cu at energies between 6 and 100 eV by Trajmar et al. [8]. Ismail and Teubner [9] reported differential cross sections and integral cross sections for the excitation of the $3d^{10}4p$ ^{2}P state in the same energy range. Madison et al. [10] reported experimental and theoretical differential cross sections for the elastic scattering of electrons from copper atoms. Their experimental measurements were performed for the energies 40, 60, 80, and 100 eV.

Theoretical calculations have been carried out by Msezane and Henry [11,12] using a four-state close-coupling calculations to study elastic scattering and excitation of the 4 ^{2}P, 3 ^{2}D and 4 ^{2}D states in the energy range of 6–100 eV. They concluded that both elastic and inelastic data of Trajmar et al. [8] should be renormalized by an energy-independent factor of 0.36. This factor was obtained by comparing their generalized oscillator strengths with those deduced from measurements of Trajmar et al. [8]. Scheibner et al. [13] carried out an R-matrix calculation for this atom at low energies, while, Scheibner and Hazi [14] extended those calculations to ten-state close-coupling and they got good agreement with the (ICS) measurements of Flynn et al. [15]. Pangantiwar and Srivastava [16] have performed a first order non-relativistic distorted-wave (DWB1) calculation for the 4 ^{2}P state up to 100 eV, while Srivastava et al. [17] included relativistic effects in their calculations for the excitation of copper from the $4s$ ground state to the $4p$ $J = 1/2$, $3/2$ fine-structure states at intermediate energies. Madison et al. [10,18] reported a first (DWB1) and a second (DWB2) order non-relativistic distorted-wave together with potential scattering differential cross sections calculations for electron copper scattering. Zhou et al. [19] used the convergent-close-coupling (CCC) and coupled-channel optical (CCO) methods to study electron scattering on the ground state of copper, using a model for

[a] e-mail: samir.al-mulla@hb.se

the target structure in which a single electron moves in the field of an inert core formed by the ten $3d$ valence electrons.

The objective of this work is to extend our previous calculations [3,6] to electron scattering from the ground state of copper for the configuration $3d^{10}4s$ and its excited state ^{2}D with the configuration $3d^9 4s^2$.

2 Theory

The procedure of calculating the potentials has been given in detail in our previous work [6]. For atomic scattering we consider two models calculations, first by using Hara exchange [4] combined together with a polarisation potential (HP). Second model (HCP) by using Hara exchange and join the correlation potential of Hedin and Lundqvist [5] with a polarisation potential. This (HCP) approach assumes high-density inhomogeneous electron gas properties for the correlation potential in the main body of the atom, and a semiclassical polarisation potential on the outlying region of the atom where the electron density is low.

For the calculation of the static and the exchange-correlation potential we have used the Hartree-Fock wavefunctions given by Clementi and Roetti [20] for all systems. For the dipole and quadrupole polarizabilities we have generalized the Kirkwood-Pople-Schofield (KPS) approach [21,22] and derived:

$$\alpha_L = -[LA_{2L-2}\mu_L^2 + (L+1)A_{2L}\nu_L^2 + 4(B_{oL}\mu_L + L(L+1)A_{2L-1}\mu_L\nu_L + B_{1L}\nu_L)/(2L+1)]$$

where $\alpha_1 = \alpha_d$, $\alpha_2 = \alpha_q$ and,

$$A_K = \left\langle \phi_o \middle| \sum_i r_i^K \middle| \phi_o \right\rangle, \quad B_{KL} = \left\langle \phi_o \middle| \sum_{i,j} r_i^K (r_i^L \cdot r_j^L) \middle| \phi_o \right\rangle \tag{1}$$

ϕ_o is approximated by a single Slater determinant and the summation is over all states in the atoms and ions. The A_K contributions involve sums of terms, each of which is associated with a single one-electron state, while the B_{KL} contains both diagonal terms ($i = j$) involving a single electron state, and non-diagonal terms ($i \neq j$) involving coupling between one-electron states of different angular momenta.

3 Results

Table 1 shows our calculations for the dipole polarizabilities α_d and the quadrupole polarizabilities α_q for copper using the KPS method. The electric dipole polarizability describes the response in lowest order of the field strength of the electron cloud to external electric field and it plays an important role in electron-atom collision processes. The KPS value for α_d (7.572 Å^3) is in the range of other theoretical and experimental values ($\alpha_d = 9$ Å^3 [23], 6.1 Å^3 [24], 9.04 Å^3 [25], 7.31 Å^3 [26]). The KPS values for α_d and α_q have been used in our calculations for the differential cross sections for copper, where the polarization potential has a large contribution to the small angle DCS.

Table 1. Dipole polarizabilities in (Å^3) and quadrupole polarizabilities in (Å^5) for copper calculated using the KPS approximation.

configurations	$3d^{10}4s$	$3d^9 4s^2$
α_d	7.572	8.976
α_q	26.70	22.35

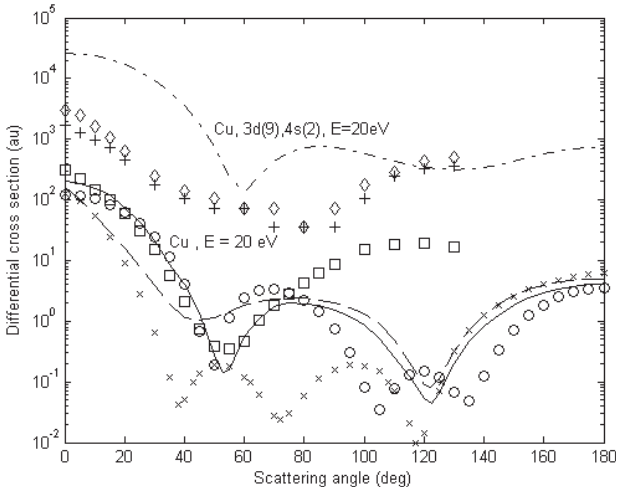

Fig. 1. Differential cross sections (a_o^2 sr^{-1}) for electron elastic scattering from copper at 20 eV. The theoretical curves are: (—) HP; (∘) HCP; (×) DWB2 of Madison et al. [10]; (- - -) potential scattering of Madison et al. [10]; (– · –) HCP (excitation). The experimental data are: (□, +) $3d^9 4s^2\ ^2\mathrm{D}_{3/2}$ and (⋄) $3d^9 4s^2\ ^2\mathrm{D}_{5/2}$ of Trajmar et al. [8]. The excitation results have been multiplied by 10^3.

Figure 1 gives results for the differential cross sections for electron scattering from copper for 20 eV incident energy. The open circle curve is the HCP model, while the solid line curve is the HP model. These results have been compared with the theoretical values of Madison et al. [10] using two model calculations (DWB2 and the potential scattering), and the experimental values of Trajmar et al. [8]. As was mentioned by Madison, there is a large difference between the DWB2 calculations and the experimental data. However, the HCP differential cross sections are in good agreement with the experimental data for scattering angles (<80°), and also with the potential scattering data of Madison et al. [10]. The HP model gives DCS in good qualitative and even quantitative agreement with the potential scattering data of Madison, while the HCP model predicts a similar structure of the DWB2 calculations.

Figure 1 also shows the HCP calculations for the DCS for the excitation state ^{2}D with the configuration $3d^9 4s^2$. These results are compared with experimental data of Trajmar et al. [8] for the $3d^9 4s^2\ ^2\mathrm{D}_{5/2}$ and the $3d^9 4s^2\ ^2\mathrm{D}_{3/2}$, where the experimental data are approximately an order of magnitude smaller.

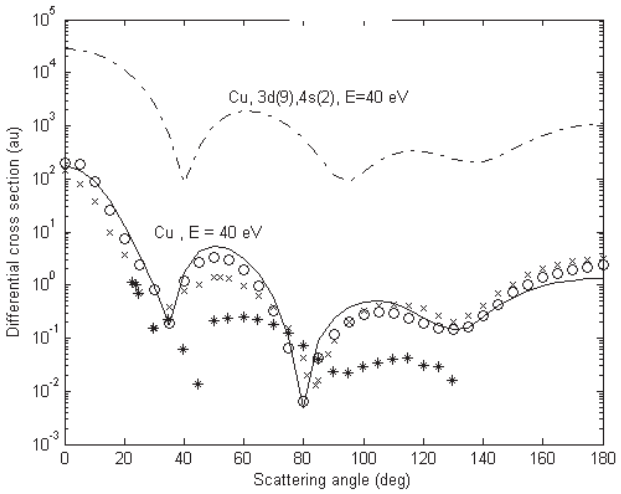

Fig. 2. Differential cross sections (a_o^2 sr^{-1}) for electron elastic scattering from copper at 40 eV. The theoretical curves are: (—) HP; (∘) HCP; (×) DWB2 of Madison et al. [10]; (– · –) HCP (excitation); (*) is the experimental data of Madison et al. [10]. The excitation results have been multiplied by 10^3.

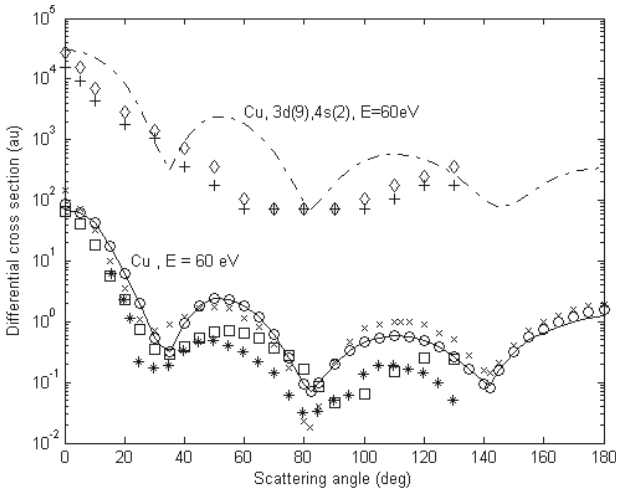

Fig. 3. Differential cross sections (a_o^2 sr^{-1}) for electron elastic scattering from copper at 60 eV. The theoretical curves are: (—) HP; (∘) HCP; (×) DWB2 of Madison et al. [10]; (– · –) HCP (excitation). The experimental data are: (□, +) $3d^9 4s^2\ ^2D_{3/2}$ and (⋄) $3d^9 4s^2\ ^2D_{5/2}$ of Trajmar et al. [8]; (*) Madison et al. [10]. The excitation results have been multiplied by 10^3.

Figure 2 compares theoretical and experimental electron-copper scattering DCS for 40 eV incident energy. Both calculations HCP and HP DCS are in good agreement with the theoretical data DWB2 of Madison et al. [10]. These calculations are also compared with the experimental data of Madison et al. [10] and both are in qualitative agreement with the measured DCS.

The HCP and the HP predict a deeper second minima shifted towards smaller angles by 5° than the DWB2 data. The $3d^9 4s^2$ DCS show similar behavior to the $3d^{10} 4s^1$ DCS, with all the three minima have been shifted by (5–10°) towards larger angles.

The agreement between the HCP and HP differential cross sections and the experimental data are improving with increasing energy as one would expect. This is shown in Figures 3, 4, and 5 for 60 eV, 80 eV and 100 eV incident electrons. Despite the differences in the absolute magnitudes, the results Hara plus correlation HCP and Hara plus polarisation HP are similar for these energies. The results from both calculations also compare fairly well with the experimental data of Trajmar et al. [8] and Madison et al. [10]. These calculations produce excellent agreement with the DWB2 data of Madison as shown in Figures 3, 4, and 5. The DCS results at 60 eV indicate that there should be a third minimum around 130–140° as was predicted by the DWB2 calculations. Despite the differences in the absolute magnitudes, the $3d^9 4s^2$ DCS are similar to the HCP and the HP calculations for the $3d^{10} 4s^1$ DCS, for all higher energies, as one would expect.

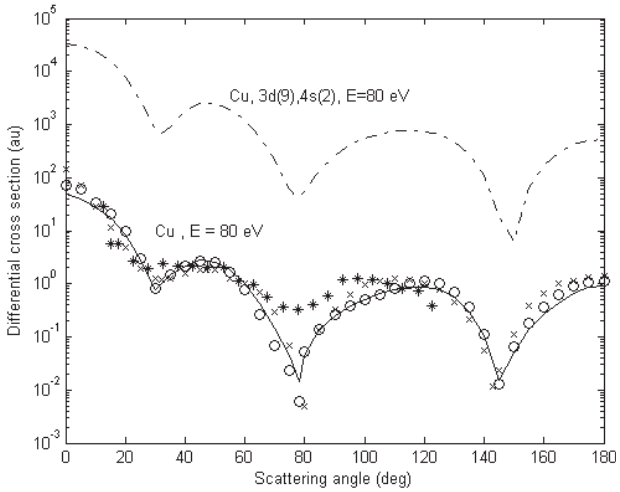

Fig. 4. Differential cross sections (a_o^2 sr^{-1}) for electron elastic scattering from copper at 80 eV. The theoretical curves are: (—) HP; (∘) HCP; (×) DWB2 of Madison et al. [10]; (– · –) HCP (excitation); (*) is the experimental data of Madison et al. [10]. The excitation results have been multiplied by 10^3.

4 Discussion and conclusions

Interest in the field of low energy scattering of electrons from copper atom has increased over recent years following experimental advances which have allowed the measurement of differential cross sections for elastic scattering. Recent calculations apply the second-order distorted-wave method. However, it is still not clear how consistently self-interaction effects are being treated. The problem is of one electron being scattered by interaction with a nucleus and N electrons, where N is far from infinite. In contrast to the N-electron ground-state problem the Hartree potential is the static electrostatic potential experienced by the scattered electron, and contains no self-interaction term requiring exact cancellation within the exchange potential. The exchange potential in turn involves interaction with $N/2$ parallel-spin electrons rather than $(N/2 - 1)$ parallel-spin electrons plus a self-interaction. Theoretically, the interaction of the electron with the target can be

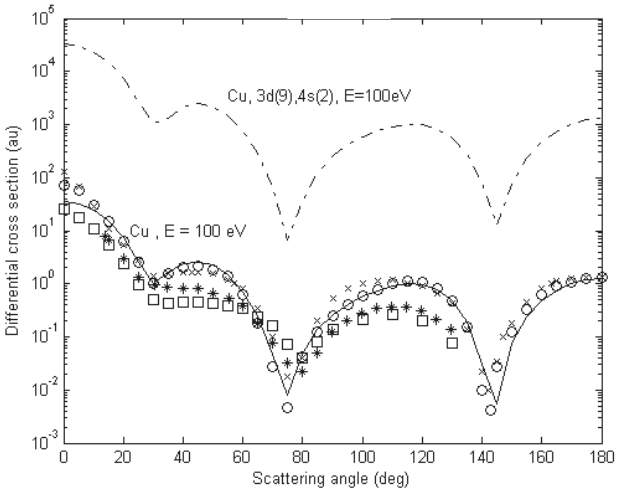

Fig. 5. Differential cross sections (a_o^2 sr^{-1}) for electron elastic scattering from copper at 100 eV. The theoretical curves are: (—) HP; (∘) HCP; (×) DWB2 of Madison et al. [10]; (– · –) HCP (excitation). The experimental data are: (□) Trajmar et al. [8]; (*) Madison et al. [10]. The excitation results have been multiplied by 10^3.

modelled using a spherically symmetric potential, which can be approximated from a Hartree-Fock-type calculation. Our early work on the elastic scattering of electrons by closed shell targets, open shell targets and positive ions show that this scattering can be well accounted for by scattering potentials derived from local-density approximations. Hara exchange with a Hedin-Lundqvist correlation potential joined to the adiabatic polarisation potential at large distance predicts phaseshifts and cross sections with a precision comparable with any non-local-density methods, even for small incident energies. This method has been used in this work for electron scattering from copper atom. As can be seen from Figure 1 for the 20 eV incident energy, except for the influence of the dominant contribution from the Coulomb field at forward angles, the shape of the differential cross sections show a good agreement with the experimental data and with the similar calculations of the potential scattering of Madison et al. [10]. The greater penetration at higher incident energy (Figs. 2, 3, 4 and 5) implies that the Hartree potential is then dominant, and the results become less sensitive to the details of the correlation and exchange potential. It might be expected that to achieve more accurate results one has to include relativistic effects.

In summary, an adequate description of the bound states in copper is essential before the various approximations are applied. An early attempts to apply the local-density approximations using the X_α potential brought the method into disrepute, but recent work and the studies presented here suggest that highly satisfactory effective scattering potential can be derived even for open shell systems such as copper by using the Hara exchange potential together with a correlation/polarisation potential which goes asymptotically to $(-\alpha_d\ /2r^4)$. Here we have shown that within the atomic radius the correlation potential may be represented by the Hedin-Lundqvist potential. Other choices of correlation potential are possible: the Perdew and Zunger [27] form is somewhat more complicated than that of Hedin and Lundqvist, but leads to very similar results. The insights obtained from this work will be used in studying the spin polarisation of electron scattering in ferromagnetic materials and to electron scattering from the excited states.

The support of the University college of Borås/College of Engineering is gratefully acknowledged.

References

1. J.A.D. Matthew, S.Y. Yousif, Surf. Science **152/153**, 38 (1985)
2. S.Y. Yousif, J.A.D. Matthew, J. Phys. B: At. Mol. Phys. **19**, 3305 (1986)
3. S.Y. Yousif Al-Mulla, L. Jönsson, Phys. Scripta **65**, 387 (2002)
4. S. Hara, J. Phys. Soc. Jap. **22**, 710 (1967)
5. L. Hedin, B.I. Lundqvist, J. Phys. C: Solid State Phys. **4**, 2064 (1971)
6. S.Y. Yousif Al-Mulla, J. Phys. B: At. Mol. Opt. Phys. **37**, 305 (2004)
7. G.J. Pert, Laser Part. Beams **12**, 209 (1994)
8. S. Trajmar, W. Williams, S.K. Srivastava, J. Phys. B: At. Mol. Phys. **10**, 3323 (1977)
9. M. Ismail, P.J.O. Teubner, J. Phys. B: At. Mol. Opt. Phys. **28**, 4149 (1995)
10. D.H. Madison, R.P. McEachran, M. Ismail, P.J.O. Teubner, J. Phys. B: At. Mol. Opt. Phys. **31**, 1127 (1998)
11. A. Msezane, R.W. Henry, Phys. Rev. A **33**, 1631 (1986)
12. A. Msezane, R.W. Henry, Phys. Rev. A **33**, 1636 (1986)
13. K.F. Scheibner, A.V. Hazi, R.J.W. Henry, Phys. Rev. A **35**, 4869 (1987)
14. K.F. Scheibner, A.V. Hazi, cited in Flynn et al. (1993)
15. C. Flynn, Z. Wei, B. Stumpf, Phys. Rev. A **48**, 1239 (1993)
16. A.W. Pangantiwar, R. Srivastava, J. Phys. B: At. Mol. Opt. Phys. **21**, 2655 (1988)
17. R. Srivastava, V. Zeman, R.P. McEachran, A. Stauffer, J. Phys. B: At. Mol. Opt. Phys. **28**, 1059 (1995)
18. D.H. Madison, J. Schroeder, K. Bartschat, R.P. McEachran, J. Phys. B: At. Mol. Opt. Phys. **28**, 4841 (1995)
19. Y. Zhou, I. Bray, I. McCarthy, J. Phys. B: At. Mol. Opt. Phys. **32**, 1033 (1999)
20. E. Clementi, C. Roetti, At. Data Nucl. Data Tables **14**, 177 (1974)
21. S.Y. Yousif Al-Mulla, Phys. Stat. Sol. (b) **240,** 99 (2003)
22. S.Y. Yousif Al-Mulla, Phys. Stat. Sol. (b) **242,** 1383 (2005)
23. R.R. Teachout, R.T. Pack, Atomic Data **3**, 195 (1971)
24. T.M. Miller, B. Bederson, Adv. At. Mol. Phys. **13**, 1 (1977)
25. S. Fraga, J. Karwowski, K.M.S. Saxena, *Handbook of Atomic Data* (Elsevier, Amsterdam, 1976)
26. H. Gollisch, J. Phys. B: At. Mol. Phys. **17**, 1463 (1984)
27. J. Perdew, A. Zunger, Phys. Rev. B **23**, 5048 (1981)